

Compensate Quantization Errors+: Quantized Models Are Inquisitive Learners

Yifei Gao¹, Jie Ou¹, Lei Wang^{2*}, Fanhua Shang³, Jaji Wu⁴, Jun Cheng²

¹University of Electronic Science and Technology of China

²Shenzhen Institutes of Advanced Technology, Chinese Academy of Sciences

³Tianjin University, ⁴Xidian University

Abstract

Large Language Models (LLMs) showcase remarkable performance and robust deductive capabilities, yet their expansive size complicates deployment and raises concerns due to substantial resource consumption. Addressing these issues, the recent development of the Learnable Singular-value Increment (LSI) technique has made strides in quantization by adjusting the hierarchy of linear weights. Nonetheless, the theoretical analysis of LSI is somewhat limited, and it does not fully address the array of “unusual performance” issues that arise. In this paper, we redefine quantization of the linear matrix as an inequality-solving challenge and improve optimization through more sophisticated weight adjustments. This is achieved by incorporating additional learnable parameters that interact with the diagonal singular-value matrix derived from the SVD of linear weights. Our approach, named **Diagonal Expansion of Learnable Singular Values (DESV)**, aligns quantization settings more effectively. Our theoretical analysis and extensive research verify the effectiveness of DESV, especially in low-bit settings. Our method consistently achieves state-of-the-art results across various quantization scenarios and demonstrates the potential for extraordinary performances in quantized models, making it suitable for broad applications.

Large language models (LLMs) have attracted considerable attention due to their exceptional performance on a variety of downstream tasks and their capability to demonstrate emergent behaviors (Bubeck et al., 2023; Touvron et al., 2023a). Furthermore, their proficiency in natural language understanding and deductive reasoning also extends to multimodal domains via alignment training (Mu et al., 2023; Xu et al., 2023; Zhang et al., 2023b). However, training and maintaining these LLMs require significant resources, often necessitating multiple GPUs to support just a single model

or its components. In this scenario, quantization becomes an essential strategy, providing solutions to decrease both the memory and computational requirements of LLMs.

In recent years, a variety of quantization methods have been developed. Quantization-Aware Training (QAT) (Liu et al., 2023a) involves adjusting the model during its training phase to enhance its compatibility with quantization techniques. On the other hand, Post-Training Quantization (PTQ) (Frantar and Alistarh, 2022a; Frantar et al., 2022; Shao et al., 2023), modifies models without the need for explicit training processes, making PTQ methods notably quicker than QAT. This advantage has led to their significant attention and broad application. Additionally, extensive research and experiments have revealed that a considerable number of errors in the quantization process stem from a few outliers with unique weight values. Addressing this, several studies (Dettmers et al., 2023b; Wei et al., 2022b, 2023; Lee et al., 2023) aim to reduce or mitigate these outliers to lessen the disturbances they create.

Recently, Learnable Singular-value Increments (LSI) is introduced (Gao et al., 2024), which integrates both transformations of weight and activation difficulties (Xiao et al., 2023; Shao et al., 2023) and the impacts of adjusting model weights (Frantar et al., 2022; Liu et al., 2023a). Meanwhile, LSI maintains a superior reference speed together with fast training process. While LSI has achieved notable results, its theoretical analysis remains lacking. Additionally, not all issues observed in their experiments have been fully addressed. For instance, the performance of quantized models may surpass that of the original models in specific downstream tasks, yet in others, they significantly lag behind.

In this paper, we explore the underlying factors contributing to the success of LSI and, based on these findings, propose a novel method, named

*Corresponding author.

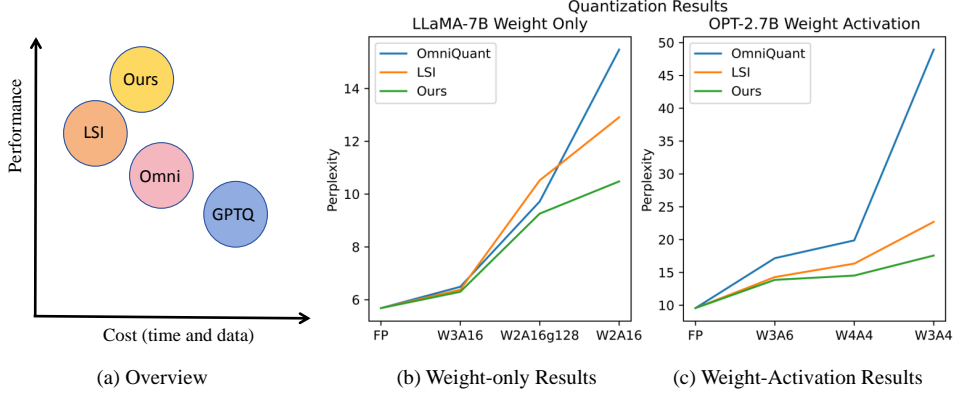


Figure 1: **Overview** of our method’s performance. (a) Our method exhibits advanced performance and compatible time consumption; (b) PPL results of LLaMA-7B in weight-only settings; (c) PPL results of OPT-2.7B in weight-activation settings.

Diagonal Expansion of Learnable Singular Values (DESV). Our method enhances the adjustment properties of LSI by cooperating more learnable parameters added on the diagonal singular-value matrix of linear weights, aiming to further unlock the potential of quantized language models. Our approach not only consistently achieves state-of-the-art results across a variety of quantization settings but also uncovers the intrinsic properties modified by quantization that enable remarkable performance on downstream tasks—a facet previously unaddressed by existing methodologies. Our contributions are summarized in the following key points:

- We are pioneers in defining the quantization of linear weight matrices as an inequality-solving problem and employing strategic methods to fully leverage its potential for achieving superior quantization results. We provide theoretical support for the enhanced adjustment abilities of our proposed DESV, and demonstrating its effectiveness.
- We conduct comprehensive experiments that illustrate the superior performance of our method, particularly in low-bit scenarios and in aligning with downstream tasks.
- We present the exceptional performances of quantized models, along with their side effects on certain downstream tasks. Additionally, we provide an analysis of how these outcomes occur and identify regular patterns, offering insights into both the strengths and limitations of these models in various applications.

1 Related Works

1.1 Quantization Methods

Uniform Quantization. Regardless of the specific methods used, the optimization objective for quantizing the weight matrix in LLMs can be uniformly expressed as follows, focusing solely on linear weight matrices:

$$\min \| \mathbf{F}(\mathbf{W}, \mathbf{X}) - \mathbf{F}(Q_w(\mathbf{W}), Q_x(\mathbf{X})) \| \quad (1)$$

In this context, \mathbf{F} represents the mapping function for a transformer block in the Large Language Model (LLM), \mathbf{W} and \mathbf{X} denote the weight and activation matrices. $Q_w(\cdot)$ and $Q_x(\cdot)$ are the quantization functions for weights and activations, respectively. Quantizers typically function by first managing the distribution of their inputs (either weights or activations) through scaling and clipping, then rounding the input to the nearest n -bit integer values:

$$Q_w(\mathbf{W}, n) = \text{Clamp}\left(\left\lfloor \frac{\mathbf{W}}{s_h} \right\rfloor + z, 0, 2^n - 1\right), \quad (2)$$

where $\text{Clamp}(\cdot)$ is a rounding function, n is the designed bit number, and s_h and z are scaler and zero point generated by specific \mathbf{W} using channel-wise scaling (Lin et al., 2023). This rounding process introduces precision loss due to the differences between the original floating-point inputs and their quantized integer counterparts. The goal of the optimization function is to minimize the discrepancy in output between the original model and its quantized version.

Smooth and Weight Clipping. The smooth technique involves modifying the magnitudes of

weights or activations by applying a scaling matrix $\text{diag}(s_c)$:

$$\mathbf{Y} = \mathbf{X}\mathbf{W} + \mathbf{B} = \underbrace{[(\mathbf{X} - \delta) \oslash s_c]}_{\tilde{\mathbf{X}}} \cdot \underbrace{[s_c \odot \mathbf{W}]}_{\tilde{\mathbf{W}}} + \underbrace{[\mathbf{B} + \delta\mathbf{W}]}_{\tilde{\mathbf{B}}}, \quad (3)$$

where \oslash and \odot denote element-wise division and multiplication, respectively; \mathbf{Y} is the final output, and \mathbf{B} is the bias. $\tilde{\mathbf{X}}$, $\tilde{\mathbf{W}}$, and $\tilde{\mathbf{B}}$ represent the equivalent activation, weight, and bias after scaling, respectively. Meanwhile, weight clipping addresses outlier issues by restricting the maximum and minimum values of weights and activations, ensuring that these values remain within a suitable range to prevent distortion in the quantized model. For more details about this approach, please refer to (Shao et al., 2023).

In OmniQuant (Shao et al., 2023), the techniques of Learnable Weight Clipping (LWC) and Learnable Equivalent Transformation (LET) are introduced to enhance the adaptability and stability of quantization processes. For LWC, the approach involves making the scaling factor s_h and the clipping bounds 0 and $2^n - 1$ in Eq. 2 into learnable parameters. Meanwhile, LET focuses on making the smooth factor s_c in Eq. 3 a learnable parameter. In our paper, we integrate both LWC and LET, combining their benefits to further refine the quantization process.

1.2 Learnable Singular-value Increment

Starting from the singular-value decomposition, LSI first decomposes a linear weight matrix $\mathbf{M} \in \mathbb{R}^{a \times b}$ (distinguished with transformer block weight \mathbf{W} and we default $a \geq b$) into three sub-matrices, $\mathbf{U} \in \mathbb{R}^{a \times a}$, $\mathbf{S} \in \mathbb{R}^b$ and $\mathbf{V} \in \mathbb{R}^{b \times b}$:

$$\begin{aligned} \mathbf{M} &= \mathbf{U} \odot \text{diag}(\mathbf{S}) \odot \mathbf{V}, \\ m_{hk} &= \sum_{j=0}^b u_{hj} s_j v_{jk}. \end{aligned} \quad (4)$$

Here, m_{hk} represents the element of the \mathbf{M} located at the h th row and k th column. $\text{diag}(\mathbf{S}) \in \mathbb{R}^{a \times b}$, is a matrix with its diagonal values equaling to \mathbf{S} . LSI incorporates an additional variable $\mathbf{I} \in \mathbb{R}^b$ that is added to the original singular values during the quantization process:

$$\begin{aligned} \mathbf{M}' &= \mathbf{U} \odot \text{diag}(\mathbf{S} + \mathbf{I}) \odot \mathbf{V}, \\ m'_{hk} &= \sum_{j=0}^b u_{hj} (s_j + i_j) v_{jk}. \end{aligned} \quad (5)$$

This modification aims to subtly alter the weight distribution of the original weight matrix \mathbf{M} into \mathbf{M}' to better suit the quantized format.

2 Our Method

In this section, we will initially simplify the quantization issues and explore them from the perspective of linear weight matrices only, and subsequently, we will demonstrate our method.

2.1 Weight Adjustment

In contemporary LLMs and transformer blocks, linear functions comprise the majority of their computational mechanisms. Thus, achieving lossless quantization of linear weight matrices could significantly reduce quantization challenges. Beyond traditional methods that primarily concentrate on the quantization process or handling outliers, LSI introduces a technique for weight adjustment that allows weights to be categorized into different hierarchies, aligning them more effectively with quantization settings. From Eq. (2), it is evident that the rounding function $[\cdot]$ grants the weight matrix \mathbf{W} the flexibility to have its elements rounded to the same value. This implies that for each element in \mathbf{W} , as long as they fall within a specific range, the rounding results will be identical. Specifically, if we assume there exists an optimal quantized weight matrix \mathbf{M}_Q for the linear weights \mathbf{M} that can be achieved through optimization, the optimization goal for the LSI technique in Eq. (5) can be redefined as an inequality-solving problem:

$$\begin{aligned} |\mathbf{M}_Q - \mathbf{M}'| &\leq \mathbf{M}_E, \\ |m_{hk}^Q - \sum_{j=0}^b u_{hj} (s_j + i_j) v_{jk}| &\leq m_{hk}^E. \end{aligned} \quad (6)$$

In this formulation, m_{hk}^Q is the element of \mathbf{M}_Q , \mathbf{M}_E represents the error matrix, where each element m^E within \mathbf{M}_E denotes the **minimum absolute value** of the solution range for each side that \mathbf{M} can introduce to achieve zero error under the quantization settings. Practically, this would encompass a wider range of values (asymmetric positive and negative ranges), but for simplicity, we only extract a subset of the possible solutions in our equations. Q is the quantizer depicted in Eq. (2). From this inequality framework, it is clear that every singular-value increment i_j in \mathbf{I} is involved in reducing the error. While the LSI technique has

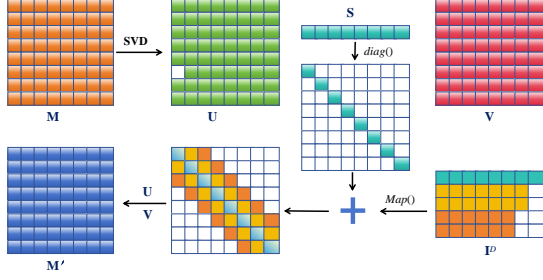


Figure 2: **Overview of DESV.** After decomposing the linear weight matrix \mathbf{M} into \mathbf{U} , \mathbf{S} , and \mathbf{V} through singular value decomposition, our technique introduces a learnable matrix \mathbf{I}^D . This matrix is then appropriately mapped into the diagonal positions of $\text{diag}(\mathbf{S})$ using the mapping function $\text{Map}(\cdot)$.

shown significant progress, as evidenced by extensive experimental results, the challenges associated with solving the inequality remain formidable. This is primarily because using less than 1% of the total parameters—often less than 0.1% in larger LLMs—to compensate for the errors in the remaining parameters is an extremely challenging task to solve the inequalities exhibited in Eq. (6), making it difficult to achieve a flawless quantization process.

2.2 Diagonal Expansion of Learnable Singular Values (DESV)

As outlined in Eq. (4) and Eq. (5), the process involves first flattening the one-dimensional vectors \mathbf{S} and \mathbf{I} into two-dimensional matrices where only the diagonal elements are populated. These diagonal matrices are then used in a multiplication process with the other two matrices, \mathbf{U} and \mathbf{V} . In our method, we concentrate on the flattened two-dimensional matrix and treat its diagonals along different axes as learnable parameters, as illustrated in Fig. 2. Building upon Eq. (5), our approach involves the diagonal expansion of learnable singular values, denoted as $\mathbf{I}^D \in \mathbb{R}^{(2n+1) \times b}$, where n represents the number of diagonals extended along both positive and negative axes. Our method encapsulates the modifications in a formulaic representation:

$$\mathbf{M}' = \mathbf{U} \odot (\text{diag}(\mathbf{S}) + \text{Map}(\mathbf{I}^D)) \odot \mathbf{V}. \quad (7)$$

In this context, $\text{Map}(\cdot)$ is a mapping function that positions the elements of \mathbf{I}^D appropriately to multi-axis diagonal elements within $\text{diag}(\mathbf{S})$. Specifically, the first row of \mathbf{I}^D is mapped onto the main diagonal, referred to as diagonal 0. Additionally, the rows at positions $2n$ and $2n + 1$ are

mapped onto the n th diagonals, which include both the upper and lower n th diagonals of the matrix. For simplicity, we combine $\text{diag}(\mathbf{S})$ and $\text{Map}(\mathbf{I}^D)$ into a single matrix $\mathbf{D} \in \mathbb{R}^{a \times b}$. Subsequently, for each d in \mathbf{D} , the element m' in \mathbf{M}' can be derived as follows:

$$m'_{hk} = \sum_{l=0}^b \sum_{j=0}^b u_{hl} d_{lj} v_{jk},$$

$$\text{where } d_{lj} = 0, \text{ if } (l < j - n) \text{ or } (l > j + n). \quad (8)$$

By incorporating the inequality-solving component from Eq. (6), the inequalities within our technique can be reformulated as follows:

$$|m'_{hk} - \sum_{l=0}^b \sum_{j=0}^b u_{hl} d_{lj}^D v_{jk}| \leq m_{hk}^E,$$

$$\text{where } d_{lj}^D = 0, \text{ if } (l < j - n) \text{ or } (l > j + n). \quad (9)$$

With the introduction of additional learnable parameters through DESV, the proposed inequalities become increasingly solvable as the expanded diagonal number n increases. Furthermore, these parameters make the \mathbf{U} component more involved, enhancing both the robustness during training and the generality during inference.

2.3 Quantization Problem Analysis

Our analysis starts with the distinct performance characteristics of quantized models employing LSI techniques. We initially observed that in some downstream tasks, these quantized models outperform their original versions. However, in others tasks, they significantly underperform compared to methods like GPTQ (Frantar et al., 2022), OmniQuant (Shao et al., 2023), and LLMQAT (Liu et al., 2023a), though they still remain competitively viable. Upon deeper investigation, we found that while these phenomena are more pronounced in the LSI series, they are not exclusive to it. These unusual outcomes, which become even more accentuated under our technique, should not be dismissed as mere anomalies. Rather, we argue that further exploration into these effects could provide deeper insights into the field. Our extensive research has revealed a similar scenario that might explain these phenomena.

We initiated our investigation by assessing the expressiveness of outputs from both original and quantized models, employing singular value decomposition to extract their singular values. Our

OPT / PPL↓	OPT-125M			OPT-1.3B			OPT-2.7B			
Task	WIKI	PT	C4	WIKI	PT	C4	WIKI	PT	C4	
FP16	-	10.86	13.09	11.74	10.13	12.34	11.20	9.56	11.84	10.69
W3A4	OmniQuant (Shao et al., 2023)	98.67	134.81	83.94	45.32	55.17	43.55	48.92	68.88	49.00
	LSI (Gao et al., 2024)	44.01	58.03	42.03	25.56	34.60	26.58	20.70	29.58	23.58
	Ours	40.96	57.21	39.79	21.53	30.54	23.40	17.57	25.70	20.13
W3A6	OmniQuant (Shao et al., 2023)	47.06	61.61	41.61	19.72	24.23	19.63	17.17	22.15	18.70
	LSI (Gao et al., 2024)	34.82	46.27	32.84	17.37	21.76	17.83	14.29	18.32	15.64
	Ours	33.70	46.27	32.18	16.69	21.10	17.37	13.87	17.97	15.34
W4A4	OmniQuant (Shao et al., 2023)	42.43	48.92	36.11	22.95	27.18	21.93	19.88	24.96	19.41
	LSI (Gao et al., 2024)	33.85	42.28	31.02	22.09	27.42	22.02	15.34	20.28	16.23
	Ours	32.73	41.80	30.36	19.19	24.88	20.98	14.52	19.65	15.77

Table 1: **Weight-activation quantization results of OPT Models.** We report perplexity on three datasets: WikiText2 (WIKI), Pen Treebank (PT), and C4. OPT-6.7B-OPT-66B results can be found in supplementary material.

OPT / PPL↓	125M	1.3B	2.7B	6.7B	13B	30B	66B
FP16	-	27.65	14.63	12.47	10.86	10.12	9.34
W2A16-g128	GPTQ (Frantar et al., 2022)	597.66	115.16	61.59	20.18	21.36	12.71
	AWQ (Lin et al., 2023)	251.84	47.97	28.50	16.20	14.32	12.31
	OmniQuant (Shao et al., 2023)	75.43	23.95	18.13	14.43	12.94	11.39
	LSI (Gao et al., 2024)	56.17	22.59	17.65	14.23	12.75	11.30
	Ours	51.40	21.39	16.97	13.88	12.58	11.18
W2A16-g64	GPTQ (Frantar et al., 2022)	204.40	49.58	29.37	16.81	16.65	11.87
	AWQ (Lin et al., 2023)	124.18	29.78	20.64	14.63	13.28	11.59
	OmniQuant (Shao et al., 2023)	62.56	21.40	16.76	13.57	12.33	11.00
	LSI (Gao et al., 2024)	50.94	21.09	16.69	13.51	12.25	10.95
	Ours	47.53	20.30	16.29	13.37	12.12	10.86
W3A16	GPTQ (Frantar et al., 2022)	53.05	21.17	16.83	15.09	11.73	10.30
	AWQ (Lin et al., 2023)	69.43	28.01	263.10	15.13	20.09	35.74
	OmniQuant (Shao et al., 2023)	35.66	16.68	13.80	11.65	10.87	10.00
	LSI (Gao et al., 2024)	32.19	16.24	13.44	11.46	10.66	9.96
	Ours	31.73	15.83	13.30	11.40	10.62	9.87

Table 2: **WikiText2 perplexity of Weight-only quantization results in OPT models.**

analysis revealed no significant differences in expressiveness among the same model families, such as LLaMA (Touvron et al., 2023a) or OPT (Zhang et al., 2022b), across three quantization methods including OmniQuant (Shao et al., 2023), LSI (Gao et al., 2024), and our own technique. Drawing on insights from LSI, which proactively introduces weight disturbances during the quantization process, we redirected our focus to examining the impact of these weight adjustments on model performance. The complete details of our experiments and more discussions are available in the Supplementary Materials.

As highlighted in (Gao et al., 2023), rescaling and rearranging attention weights—a type of weight disturbance—can enhance or impair specific capabilities of LLMs. Our quantization approach, detailed in Eq. (6) and Eq. (9), allows for modifications in weight without introducing additional errors. Furthermore, the integration of \mathbf{I} and \mathbf{I}^D enhances the flexibility of weight hierarchies and magnitudes. Unlike the hand-crafted GPTQ series (Frantar et al., 2022; Lin et al., 2023; Dettmers

et al., 2023b), our parameters are more adaptable, as the training procedures are fully dependent on aligning data during training, allowing for more dynamic adjustments. Therefore, our technique can effectively adjust model weights to better align with specific tasks, enhancing certain properties while dampening others. We refer to these quantized LLMs as ‘*Inquisitive Learners*’. Given the appropriate materials for alignment, these models can perform exceptionally well under designed conditions.

3 Experiments

3.1 Settings

Quantization. Our experiments encompass both weight-only and weight-activation quantization scenarios, and we present some results using low-bit configurations. In these configurations, ‘W’ denotes *weight* and ‘A’ indicates *activation*. When employing group-wise scaling, as discussed in (Frantar et al., 2022; Dettmers et al., 2023b), where each group is assigned unique quantization parameters, ‘g’ represents the group name. To minimize

Acc \uparrow	Method	ARC-E	ARC-C	Boolq	PIQA	WG	HS	Avg.
OPT-1.3B	FP16	57.19	23.37	57.70	71.76	59.35	41.55	51.82
	OmniQuant (Shao et al., 2023)	49.45	22.09	52.99	65.83	51.69	35.64	46.28
	LSI (Gao et al., 2024)	49.94	22.71	53.43	66.02	52.31	36.05	46.74
	Ours	50.58	23.03	54.12	66.81	52.64	36.43	47.26
OPT-2.7B	FP16	60.73	26.87	60.30	73.77	61.01	45.83	54.75
	OmniQuant (Shao et al., 2023)	49.28	21.50	54.06	66.15	52.24	37.91	46.85
	LSI (Gao et al., 2024)	55.13	26.19	56.08	70.56	54.61	41.74	50.71
	Ours	56.86	26.02	57.90	70.89	56.51	42.11	51.71
OPT-6.7B	FP16	65.61	30.63	66.14	76.27	65.50	50.45	59.10
	OmniQuant (Shao et al., 2023)	62.83	28.66	60.70	75.13	61.02	47.95	56.07
	LSI (Gao et al., 2024)	63.71	29.24	61.45	74.10	60.45	47.74	56.11
	Ours	64.68	29.01	62.96	75.22	61.72	48.54	57.02
OPT-13B	FP16	67.12	32.93	65.84	76.00	64.95	52.44	59.88
	OmniQuant (Shao et al., 2023)	57.40	26.19	47.79	70.23	57.69	38.68	49.66
	LSI (Gao et al., 2024)	58.33	25.85	49.17	68.87	58.16	41.05	50.23
	Ours	59.24	28.15	52.07	70.34	61.72	41.53	52.17
OPT-30B	FP16	70.11	34.55	70.42	77.63	68.19	54.30	62.65
	OmniQuant (Shao et al., 2023)	67.12	32.50	64.49	75.84	62.03	50.93	58.81
	LSI (Gao et al., 2024)	67.92	28.37	66.28	76.21	64.13	51.24	59.02
	Ours	68.75	32.97	67.06	76.44	65.74	51.98	60.49

Table 3: **Downstream tasks of OPT Models.** We report the W4A4 accuracy (\uparrow) of 6 zero-shot tasks compared with other baselines. The training data is selected from WikiText2.

disruptions during quantization, we retained the *Softmax* component in float32.

Training. Our training configurations are generally the same as the LSI (Gao et al., 2024). In addition, LET and LWC (Gao et al., 2024; Shao et al., 2023) are also incorporated during training. We initialize our scaling and shifting parameters from (Shao et al., 2023) and keep their learning rates as in (Shao et al., 2023), then we train DESV parameters with a low learning rate at $1.5e-4$. We employ the AdamW (Loshchilov and Hutter, 2019) optimizer with a weight decay of 0 to optimize our parameters. The data used in our training was collected from WikiText2 (Merity et al., 2016) and C4 (Raffel et al., 2020). For expanded diagonal number n , we consistently set it to 100. The increase of n will introduce additional training time but without significant enhancement of model performance, and 100 is just enough through our tests.

Models. We conduct evaluation on two popular baselines for generalization, LLaMA (7-30B) (Touvron et al., 2023a) and OPT (125M-66B) (Zhang et al., 2022b) for generalization. For comprehensive experimental results, please see the supplementary materials.

Evaluation. Our evaluation of perplexity primarily focuses on the WikiText-2 (Merity et al., 2016), PTB (Marcus et al., 1994), and C4 (Raffel et al., 2020) datasets. Additionally, in line with prior research, we assess several zero-shot tasks within a weight-activation quantization setting, including PIQA (Bisk et al., 2020), ARC (ARC-

E and ARC-C) (Clark et al., 2018), HellaSwag (HS) (Zellers et al., 2019), GLUE (RTE, QQP, MRPC) (Wang et al., 2018), WIC (Wang et al., 2019), COQA (Reddy et al., 2018), Winogrande (WG) (Sakaguchi et al., 2019) and Boolq (Clark et al., 2019). The datasets selected for evaluation adhere to the GPTQ (Frantar et al., 2022) guidelines. For measuring accuracy in these zero-shot tasks, we utilize the lm-eval-harness (Gao et al., 2021).

Baselines. For weight-only quantization, we select the previously state-of-the-art methods AWQ (Lin et al., 2023), OmniQuant (Shao et al., 2023), and the more recent LSI (Gao et al., 2024) as our baselines. In the weight-activation quantization category, we select both Quantization Aware Training (QAT) and Post-Training Quantization (PTQ) methods, featuring RPTQ (Yuan et al., 2023), QAT (Liu et al., 2023a), OmniQuant (Shao et al., 2023), and LSI (Gao et al., 2024). Consistent with the approach outlined in SmoothQuant (Xiao et al., 2023), we maintain the per-channel quantization strategy for weights and the per-tensor strategy for activations.

3.2 Weight-only and Weight-activation Quantization Results

In this section, we present the results of the OPT series in low-bit settings on Perplexity, as detailed in Tables 1 and 2. The results demonstrate that DESV offers more effective and powerful quantization solutions for LLMs than previous methods under

PPL↓/ Acc↑	#Bits	Method	Wiki	C4	Boolq	PIQA	COQA	WG	RTE	Avg.
LLaMA-7B	FP16	-	-	-	73.08	77.47	85.00	67.07	53.42	71.20
	W4A4	SmoothQuant (Xiao et al., 2023)	-	-	49.10	49.80	58.00	48.00	45.32	49.90
	W4A4	LLM-QAT+SQ (Liu et al., 2023a)	-	-	62.40	55.90	62.00	50.60	47.61	55.70
	W4A4	OmniQuant (Shao et al., 2023)	11.26	14.51	63.51	66.15	75.00	53.43	50.18	61.65
	W4A4	LSI (Gao et al., 2024)	11.02	13.77	62.19	67.90	76.00	56.27	54.59	63.39
	W4A4	Ours-Wiki	10.21	13.18	62.47	68.71	77.00	57.14	52.70	63.61
	W4A4	Ours-C4	10.83	12.94	64.61	69.47	72.00	55.80	51.62	62.70
LLaMA-13B	FP16	-	-	-	68.01	79.10	90.00	70.31	65.34	74.55
	W4A4	OmniQuant (Shao et al., 2023)	10.87	13.78	62.84	69.69	83.00	55.80	54.51	65.17
	W4A4	LSI (Gao et al., 2024)	10.68	12.84	64.04	69.69	87.00	59.59	54.87	67.03
	W4A4	Ours-Wiki	9.72	12.51	64.74	70.73	87.00	58.24	56.34	67.41
	W4A4	Ours-C4	10.00	12.14	63.85	71.87	85.00	60.45	53.79	66.99
LLaMA-30B	FP16	-	-	-	68.44	80.08	90.00	72.53	61.37	74.48
	W4A4	OmniQuant (Shao et al., 2023)	10.33	12.49	65.33	71.21	83.00	59.19	53.79	66.50
	W4A4	LSI (Gao et al., 2024)	10.20	12.12	65.95	73.17	86.00	60.22	54.35	67.93
	W4A4	Ours-Wiki	9.12	11.71	65.91	73.62	87.00	62.17	55.82	68.91
	W4A4	Ours-C4	9.54	11.37	66.54	73.98	85.00	64.55	54.29	68.82

Table 4: **Downstream tasks of LLaMA Models.** We report the PPL (\downarrow) of Wikitext2 and C4 together with the accuracy (\uparrow) of 5 zero-shot tasks compared with other baselines.

similar conditions. Particularly, in low-bit weight-activation quantization, methods from the LSI series exhibit notably strong performance. However, while the LSI performs stable within the OPT family, it tends to experience performance degradation in the LLaMA family, where outliers and weight hierarchies are more sensitive (Shao et al., 2023; Gao et al., 2024), even when initiated with well-trained OmniQuant parameters. With more learnable parameters for adjustments compared to LSI, our methods consistently exhibit stable and outstanding results compared with previous methods. Our complete results are available in the supplementary material.

3.3 Quantization Results of Downstream Tasks

In this section, we showcase the performance of various downstream tasks using the OPT and LLaMA series, detailed in Tables 3 and 4. Our results highlight some improvements compared to previous methods and the improvements are more evident for bigger models. Moreover, different aligning datasets could also enhance various model properties, each providing unique advantages as shown in Table 4. While our method yields significant improvements in perplexity, amplifying one aspect of performance can also lead to a reduction in another. This is particularly prominent when it comes to LLaMA families, as the weight distribution is more aggregated compared with the OPT families.

From a compromise perspective, instead of viewing these variations as drawbacks, we can leverage our technique across a broader range of appli-

cations to demonstrate its potential benefits. As shown in Table 5, DESV can significantly outperform the original model in the **Advanced** parts, facilitating the implementation of our technique.

3.4 Performance Analysis

After observing the exceptional results of quantization models, we sought to identify a regular pattern to better explain this phenomenon. Initially, it is important to recognize that quantization compromises the robustness of the model to decrease its memory footprint. Specifically, the rounding behavior of the quantization tends to diminish the disparity of information conveyed in the hidden states of the model. From this, we deduce that the simplification of information complexity in the outputs of quantized models leads to improved performance in certain downstream tasks. In essence, quantization aids the model by filtering out extraneous information in some downstream tasks, making the model more effective in handling simpler and more straightforward tasks. Applying this insight to tasks like ARC-E and QQP, we find that it aligns well with the simplicity and straightforward format of these datasets.

On the other hand, despite the inherent reductions associated with quantization, both LSI (Gao et al., 2024) and our methods experience significant performance drops in some downstream tasks, particularly with the LLaMA series. Our analysis revealed that tasks like AEC-C and HS often involve key words with specific meanings or contextual significance crucial for deriving accurate answers. For instance, in the question, “Which of

Model	LLaMA-7B						OPT-2.7B	
Results	Advanced			Degraded			Advanced	
Method	ARC-E	WIC	QQP	ARC-C	MRPC	HS	MRPC	QQP
Original	52.48	50.00	36.83	41.46	68.38	73.00	67.64	43.29
OmniQuant (Shao et al., 2023)	45.20	51.25	41.90	31.14	60.29	56.44	51.22	39.99
LSI (Gao et al., 2024)	56.14	50.78	43.23	31.39	49.85	48.17	66.17	39.60
Ours	56.32	51.25	44.41	30.73	47.30	47.16	67.74	46.51

Model	LLaMA-13B						OPT-13B	
Results	Advanced			Degraded			Advanced	
Method	ARC-E	WIC	QQP	ARC-C	MRPC	HS	MRPC	QQP
Original	59.89	50.00	36.78	44.45	68.62	76.21	41.17	57.08
OmniQuant (Shao et al., 2023)	47.39	46.39	41.16	33.10	51.22	58.96	46.07	49.80
LSI (Gao et al., 2024)	57.99	49.85	43.97	31.39	49.85	48.17	61.51	47.54
Ours	61.05	50.96	45.08	30.73	47.30	47.16	60.28	59.36

Table 5: Downstream tasks with advanced or degraded outcomes. All these results are in the W4A4 setting.

the following statements best explains why magnets usually stick to a refrigerator door," the words "magnets" and "stick" are pivotal. Quantization, by smoothing information processing, can diminish the model's ability to emphasize such critical terms, potentially leading to decreased accuracy in these contexts. Moreover, the significant weight adjustments introduced by our method tend to amplify existing issues. We analyzed the accumulated attention weights in the first layer's attention mechanism of the quantized LLaMA-7B, comparing our method to the original model. We observed that the attention weights on critical terms like 'magnets' and 'stick' decreased significantly, by approximately 1/6 and 1/5 respectively, while the attention weight on 'refrigerator' increased by about 1/5. In contrast, another quantization method, OmniQuant (Shao et al., 2023), exhibited variations of no greater than 1/8 in these weights.

Although these findings are not definitive enough to establish a clear relationship between the specific weight adjustments made by our method and the observed drop in performance, they do suggest that our weight adjustments might not be well-suited for deployment in 'sensitive models' tackling complex and nuanced tasks. But in general, our methods are competitive enough to achieve comprehensive success not only in PPL evaluation but also the performance of most downstream tasks.

4 Further Discussions

4.1 Inference Speed

During the inference procedure, DESV does not introduce additional operations or parameters compared to OmniQuant (Shao et al., 2023). We also adhere to the criteria proposed by MCL-LLM*, which focuses on versatile deployment solutions

*<https://github.com/mlc-ai/mlc-llm>

Bits	LLaMA-7B		
	WM	RM	token/s
FP	12.6G	14.4G	69.2
W3A16g128	3.2G	5.2G	83.1
W2A16g128	2.2G	4.1G	84.2

Bits	LLaMA-13B		
	WM	RM	token/s
FP	24.3G	27.1G	52.5
W3A16g128	5.8G	8.8G	56.9
W2A16g128	4.0G	7.5G	93.1

Table 6: Deployment of weight-only quantization through MLC-LLM. We report the memory size of quantized weights (denoted as 'WM') and the running memory (denoted as 'RM') and speed in NVIDIA A100-80G.

for diverse language models across various hardware platforms. The inference speed, demonstrated in Table 6, shows only minor variations compared to OmniQuant, further proving the conciseness and simplicity of our technique during inference.

4.2 Performance Degradation

As previously suggested, our technique enhances certain model properties at the cost of others. This trade-off is evident in the **Degraded** part in Table 5, where our method shows significant accuracy degradation but still maintains a competitive accuracy norm. Notably, clear degradation is observed primarily in the LLaMA families. In contrast, for the OPT families, which have more distinct and robust weights, the degradation is minimal. Our extensive experiments also reveal that this polarization is consistent in the W6A6 setting, although it becomes negligible in the W8A8 setting where quantization errors are minimal.

4.3 Training Variations

Through our experiments, we found that our technique offer greater stability compared to LSI (Gao et al., 2024) when used in weight-only and high-

bit weight-activation quantization settings. However, in low-bit weight-activation scenarios such as W4A6 and W4A4, we observe performance fluctuations in downstream tasks, especially in LLaMA families. Notably, in tasks like PIQA and Boolq, these fluctuations can reach up to ± 2.5 , impacting the stability of results across other tasks as well. In our paper, we present balanced outcomes rather than these *extreme* results. Additionally, the results displayed in Table 5 derive from the same models shown in Tables 3 and 4, which were trained on WikiText2.

5 Conclusion

We introduce **DESV** to optimize data alignment across various quantization settings, achieving state-of-the-art performance in diverse scenarios. Notably, in low-bit settings, our results significantly outperform that of previous methods. Furthermore, our technique occasionally exceeds the performance of the original models in certain downstream tasks, though it sometimes also introduces substantial degradation in others in some weights-sensitive models. We believe that by fully harnessing the potential of our technique, this polarized characteristic can be effectively utilized across a broad spectrum of applications.

References

- Alfred V. Aho and Jeffrey D. Ullman. 1972. *The Theory of Parsing, Translation and Compiling*, volume 1. Prentice-Hall, Englewood Cliffs, NJ.
- American Psychological Association. 1983. *Publications Manual*. American Psychological Association, Washington, DC.
- Rie Kubota Ando and Tong Zhang. 2005. A framework for learning predictive structures from multiple tasks and unlabeled data. *Journal of Machine Learning Research*, 6:1817–1853.
- Galen Andrew and Jianfeng Gao. 2007. Scalable training of L1-regularized log-linear models. In *Proceedings of the 24th International Conference on Machine Learning*, pages 33–40.
- Ron Banner, Itay Hubara, Elad Hoffer, and Daniel Soudry. 2018. Scalable methods for 8-bit training of neural networks. *Advances in neural information processing systems*, 31.
- Yoshua Bengio and Yann LeCun. 2007. Scaling learning algorithms towards AI. In *Large Scale Kernel Machines*. MIT Press.
- Yonatan Bisk, Rowan Zellers, Jianfeng Gao, Yejin Choi, et al. 2020. Piqa: Reasoning about physical commonsense in natural language. In *Proceedings of the AAAI conference on artificial intelligence*, volume 34, pages 7432–7439.
- Tom Brown, Benjamin Mann, Nick Ryder, Melanie Subbiah, Jared D Kaplan, Prafulla Dhariwal, Arvind Neelakantan, Pranav Shyam, Girish Sastry, Amanda Askell, et al. 2020. Language models are few-shot learners. *Advances in neural information processing systems*, 33:1877–1901.
- Sébastien Bubeck, Varun Chandrasekaran, Ronen Eldan, Johannes Gehrke, Eric Horvitz, Ece Kamar, Peter Lee, Yin Tat Lee, Yuanzhi Li, Scott Lundberg, et al. 2023. Sparks of artificial general intelligence: Early experiments with gpt-4. *arXiv preprint arXiv:2303.12712*.
- Yuji Chai, John Gkountouras, Glenn G Ko, David Brooks, and Gu-Yeon Wei. 2023. Int2. 1: Towards fine-tunable quantized large language models with error correction through low-rank adaptation. *arXiv preprint arXiv:2306.08162*.
- Ashok K. Chandra, Dexter C. Kozen, and Larry J. Stockmeyer. 1981. *Alternation*. *Journal of the Association for Computing Machinery*, 28(1):114–133.
- Jerry Chee, Yaohui Cai, Volodymyr Kuleshov, and Christopher De Sa. 2023. Quip: 2-bit quantization of large language models with guarantees. *arXiv preprint arXiv:2307.13304*.
- Wei-Lin Chiang, Zhuohan Li, Zi Lin, Ying Sheng, Zhanghao Wu, Hao Zhang, Lianmin Zheng, Siyuan Zhuang, Yonghao Zhuang, Joseph E. Gonzalez, Ion Stoica, and Eric P. Xing. 2023. *Vicuna: An open-source chatbot impressing gpt-4 with 90%* chatgpt quality*.
- Jungwook Choi, Zhuo Wang, Swagath Venkataramani, Pierce I-Jen Chuang, Vijayalakshmi Srinivasan, and Kailash Gopalakrishnan. 2018. Pact: Parameterized clipping activation for quantized neural networks. *arXiv preprint arXiv:1805.06085*.
- Christopher Clark, Kenton Lee, Ming-Wei Chang, Tom Kwiatkowski, Michael Collins, and Kristina Toutanova. 2019. Boolq: Exploring the surprising difficulty of natural yes/no questions. *arXiv preprint arXiv:1905.10044*.
- Peter Clark, Isaac Cowhey, Oren Etzioni, Tushar Khot, Ashish Sabharwal, Carissa Schoenick, and Oyvind Tafjord. 2018. Think you have solved question answering? try arc, the ai2 reasoning challenge. *arXiv preprint arXiv:1803.05457*.
- Tim Dettmers, Mike Lewis, Younes Belkada, and Luke Zettlemoyer. 2022. Llm.int8(): 8-bit matrix multiplication for transformers at scale. *arXiv preprint arXiv:2208.07339*.

- Tim Dettmers, Artidoro Pagnoni, Ari Holtzman, and Luke Zettlemoyer. 2023a. Qlora: Efficient finetuning of quantized llms. *arXiv preprint arXiv:2305.14314*.
- Tim Dettmers, Ruslan Svirschevski, Vage Egiazarian, Denis Kuznedelev, Elias Frantar, Saleh Ashkboos, Alexander Borzunov, Torsten Hoefler, and Dan Alistarh. 2023b. Spqr: A sparse-quantized representation for near-lossless llm weight compression. *arXiv preprint arXiv:2306.03078*.
- Tim Dettmers and Luke Zettlemoyer. 2023. The case for 4-bit precision: k-bit inference scaling laws. In *International Conference on Machine Learning*, pages 7750–7774. PMLR.
- Jacob Devlin, Ming-Wei Chang, Kenton Lee, and Kristina Toutanova. 2018. Bert: Pre-training of deep bidirectional transformers for language understanding. *arXiv preprint arXiv:1810.04805*.
- Steven K Esser, Jeffrey L McKinstry, Deepika Bablani, Rathinakumar Appuswamy, and Dharmendra S Modha. 2019. Learned step size quantization. *arXiv preprint arXiv:1902.08153*.
- Julian Faraone, Nicholas Fraser, Michaela Blott, and Philip HW Leong. 2018. Syq: Learning symmetric quantization for efficient deep neural networks. In *Proceedings of the IEEE Conference on Computer Vision and Pattern Recognition*, pages 4300–4309.
- Elias Frantar and Dan Alistarh. 2022a. Optimal brain compression: A framework for accurate post-training quantization and pruning. *Advances in Neural Information Processing Systems*, 35:4475–4488.
- Elias Frantar and Dan Alistarh. 2022b. Optimal brain compression: A framework for accurate post-training quantization and pruning. *Advances in Neural Information Processing Systems*, 35:4475–4488.
- Elias Frantar, Saleh Ashkboos, Torsten Hoefler, and Dan Alistarh. 2022. Gptq: Accurate post-training quantization for generative pre-trained transformers. *arXiv preprint arXiv:2210.17323*.
- Leo Gao, Stella Biderman, Sid Black, Laurence Golding, Travis Hoppe, Charles Foster, Jason Phang, Ho-race He, Anish Thite, Noa Nabeshima, et al. 2020. The pile: An 800gb dataset of diverse text for language modeling. *arXiv preprint arXiv:2101.00027*.
- Leo Gao, Jonathan Tow, Stella Biderman, Sid Black, Anthony DiPofi, Charles Foster, Laurence Golding, Jeffrey Hsu, Kyle McDonell, Niklas Muennighoff, et al. 2021. A framework for few-shot language model evaluation. *Version v0. 0.1. Sept*.
- Yifei Gao, Jie Ou, Lei Wang, Yuting Xiao, Zhiyuan Xiang, Ruiting Dai, and Jun Cheng. 2024. [Compensate quantization errors: Make weights hierarchical to compensate each other.](#)
- Yifei Gao, Lei Wang, Jun Fang, Longhua Hu, and Jun Cheng. 2023. Empower your model with longer and better context comprehension. *arXiv preprint arXiv:2307.13365*.
- Ian Goodfellow, Yoshua Bengio, Aaron Courville, and Yoshua Bengio. 2016. *Deep learning*, volume 1. MIT Press.
- Cong Guo, Chen Zhang, Jingwen Leng, Zihan Liu, Fan Yang, Yunxin Liu, Minyi Guo, and Yuhao Zhu. 2022. Ant: Exploiting adaptive numerical data type for low-bit deep neural network quantization. In *2022 55th IEEE/ACM International Symposium on Microarchitecture (MICRO)*, pages 1414–1433. IEEE.
- Dan Gusfield. 1997. *Algorithms on Strings, Trees and Sequences*. Cambridge University Press, Cambridge, UK.
- Ruidan He, Linlin Liu, Hai Ye, Qingyu Tan, Bosheng Ding, Liying Cheng, Jia-Wei Low, Lidong Bing, and Luo Si. 2021. On the effectiveness of adapter-based tuning for pretrained language model adaptation. *arXiv preprint arXiv:2106.03164*.
- Dan Hendrycks, Collin Burns, Steven Basart, Andy Zou, Mantas Mazeika, Dawn Song, and Jacob Steinhardt. 2020. Measuring massive multitask language understanding. *arXiv preprint arXiv:2009.03300*.
- Geoffrey E. Hinton, Simon Osindero, and Yee Whye Teh. 2006. A fast learning algorithm for deep belief nets. *Neural Computation*, 18:1527–1554.
- Jonathan Ho, Ajay Jain, and Pieter Abbeel. 2020. Denoising diffusion probabilistic models. *Advances in neural information processing systems*, 33:6840–6851.
- Lu Hou, Zhiqi Huang, Lifeng Shang, Xin Jiang, Xiao Chen, and Qun Liu. 2020. Dynabert: Dynamic bert with adaptive width and depth. *Advances in Neural Information Processing Systems*, 33:9782–9793.
- Edward J Hu, Yelong Shen, Phillip Wallis, Zeyuan Allen-Zhu, Yuanzhi Li, Shean Wang, Lu Wang, and Weizhu Chen. 2021. Lora: Low-rank adaptation of large language models. *arXiv preprint arXiv:2106.09685*.
- Zhiqiang Hu, Yihuai Lan, Lei Wang, Wanyu Xu, Ee-Peng Lim, Roy Ka-Wei Lee, Lidong Bing, and Soujanya Poria. 2023. Llm-adapters: An adapter family for parameter-efficient fine-tuning of large language models. *arXiv preprint arXiv:2304.01933*.
- Itay Hubara, Yury Nahshan, Yair Hanani, Ron Banner, and Daniel Soudry. 2020. Improving post training neural quantization: Layer-wise calibration and integer programming. *arXiv preprint arXiv:2006.10518*.
- Benoit Jacob, Skirmantas Kligys, Bo Chen, Menglong Zhu, Matthew Tang, Andrew Howard, Hartwig Adam, and Dmitry Kalenichenko. 2018. Quantization and training of neural networks for efficient

- integer-arithmetic-only inference. In *Proceedings of the IEEE conference on computer vision and pattern recognition*, pages 2704–2713.
- Sehoon Kim, Amir Gholami, Zhewei Yao, Michael W Mahoney, and Kurt Keutzer. 2021. I-bert: Integer-only bert quantization. In *International conference on machine learning*, pages 5506–5518. PMLR.
- Raghuraman Krishnamoorthi. 2018. Quantizing deep convolutional networks for efficient inference: A whitepaper. *arXiv preprint arXiv:1806.08342*.
- Changhun Lee, Jungyu Jin, Taesu Kim, Hyungjun Kim, and Eunhyeok Park. 2023. Owq: Lessons learned from activation outliers for weight quantization in large language models. *arXiv preprint arXiv:2306.02272*.
- Yuhang Li, Ruihao Gong, Xu Tan, Yang Yang, Peng Hu, Qi Zhang, Fengwei Yu, Wei Wang, and Shi Gu. 2021. Brecq: Pushing the limit of post-training quantization by block reconstruction. *arXiv preprint arXiv:2102.05426*.
- Ji Lin, Jiaming Tang, Haotian Tang, Shang Yang, Xingyu Dang, and Song Han. 2023. Awq: Activation-aware weight quantization for llm compression and acceleration. *arXiv preprint arXiv:2306.00978*.
- Zechun Liu, Kwang-Ting Cheng, Dong Huang, Eric P Xing, and Zhiqiang Shen. 2022. Nonuniform-to-uniform quantization: Towards accurate quantization via generalized straight-through estimation. In *Proceedings of the IEEE/CVF Conference on Computer Vision and Pattern Recognition*, pages 4942–4952.
- Zechun Liu, Barlas Oguz, Changsheng Zhao, Ernie Chang, Pierre Stock, Yashar Mehdad, Yangyang Shi, Raghuraman Krishnamoorthi, and Vikas Chandra. 2023a. Llm-qat: Data-free quantization aware training for large language models. *arXiv preprint arXiv:2305.17888*.
- Zichang Liu, Jue Wang, Tri Dao, Tianyi Zhou, Binhang Yuan, Zhao Song, Anshumali Shrivastava, Ce Zhang, Yuandong Tian, Christopher Re, et al. 2023b. Dejavu: Contextual sparsity for efficient llms at inference time. In *International Conference on Machine Learning*, pages 22137–22176. PMLR.
- Ilya Loshchilov and Frank Hutter. 2019. Decoupled weight decay regularization. In *The International Conference on Learning Representations (ICLR)*.
- Mitch Marcus, Grace Kim, Mary Ann Marcinkiewicz, Robert MacIntyre, Ann Bies, Mark Ferguson, Karen Katz, and Britta Schasberger. 1994. The penn treebank: Annotating predicate argument structure. In *Human Language Technology: Proceedings of a Workshop held at Plainsboro, New Jersey, March 8-11, 1994*.
- Julieta Martinez, Shobhit Zakhmi, Holger H Hoos, and James J Little. 2018. Lsq++: Lower running time and higher recall in multi-codebook quantization. In *Proceedings of the European Conference on Computer Vision (ECCV)*, pages 491–506.
- Stephen Merity, Caiming Xiong, James Bradbury, and Richard Socher. 2016. Pointer sentinel mixture models. *arXiv preprint arXiv:1609.07843*.
- Yao Mu, Qinglong Zhang, Mengkang Hu, Wenhai Wang, Mingyu Ding, Jun Jin, Bin Wang, Jifeng Dai, Yu Qiao, and Ping Luo. 2023. Embodiedgpt: Vision-language pre-training via embodied chain of thought. *arXiv preprint arXiv:2305.15021*.
- Markus Nagel, Rana Ali Amjad, Mart Van Baalen, Christos Louizos, and Tijmen Blankevoort. 2020. Up or down? adaptive rounding for post-training quantization. In *International Conference on Machine Learning*, pages 7197–7206. PMLR.
- Markus Nagel, Marios Fournarakis, Rana Ali Amjad, Yelysei Bondarenko, Mart Van Baalen, and Tijmen Blankevoort. 2021. A white paper on neural network quantization. *arXiv preprint arXiv:2106.08295*.
- Gunho Park, Baeseong Park, Se Jung Kwon, Byeongwook Kim, Youngjoo Lee, and Dongsoo Lee. 2022a. nuqmm: Quantized matmul for efficient inference of large-scale generative language models. *arXiv preprint arXiv:2206.09557*.
- Minseop Park, Jaeseong You, Markus Nagel, and Simyung Chang. 2022b. Quadapter: Adapter for gpt-2 quantization. *arXiv preprint arXiv:2211.16912*.
- Guilherme Penedo, Quentin Malartic, Daniel Hesslow, Ruxandra Cojocaru, Alessandro Cappelli, Hamza Alobeidli, Baptiste Pannier, Ebtesam Almazrouei, and Julien Launay. 2023. The refinedweb dataset for falcon llm: outperforming curated corpora with web data, and web data only. *arXiv preprint arXiv:2306.01116*.
- Colin Raffel, Noam Shazeer, Adam Roberts, Katherine Lee, Sharan Narang, Michael Matena, Yanqi Zhou, Wei Li, and Peter J Liu. 2020. Exploring the limits of transfer learning with a unified text-to-text transformer. *The Journal of Machine Learning Research*, 21(1):5485–5551.
- Mohammad Sadegh Rasooli and Joel R. Tetreault. 2015. *Yara parser: A fast and accurate dependency parser*. *Computing Research Repository*, arXiv:1503.06733. Version 2.
- Siva Reddy, Danqi Chen, and Christopher D. Manning. 2018. *Coqa: A conversational question answering challenge*.
- Andreas Rücklé, Gregor Geigle, Max Glockner, Tilman Beck, Jonas Pfeiffer, Nils Reimers, and Iryna Gurevych. 2020. Adapterdrop: On the efficiency of adapters in transformers. *arXiv preprint arXiv:2010.11918*.

- Keisuke Sakaguchi, Ronan Le Bras, Chandra Bhagavatula, and Yejin Choi. 2019. Winogrande: An adversarial winograd schema challenge at scale. *arXiv preprint arXiv:1907.10641*.
- Keisuke Sakaguchi, Ronan Le Bras, Chandra Bhagavatula, and Yejin Choi. 2021. Winogrande: An adversarial winograd schema challenge at scale. *Communications of the ACM*, 64(9):99–106.
- Teven Le Scao, Angela Fan, Christopher Akiki, Ellie Pavlick, Suzana Ilić, Daniel Hesslow, Roman Castagné, Alexandra Sasha Luccioni, François Yvon, Matthias Gallé, et al. 2022. Bloom: A 176b-parameter open-access multilingual language model. *arXiv preprint arXiv:2211.05100*.
- Wenqi Shao, Mengzhao Chen, Zhaoyang Zhang, Peng Xu, Lirui Zhao, Zhiqian Li, Kaipeng Zhang, Peng Gao, Yu Qiao, and Ping Luo. 2023. Omniquant: Omnidirectionally calibrated quantization for large language models. *arXiv preprint arXiv:2308.13137*.
- Sheng Shen, Zhen Dong, Jiayu Ye, Linjian Ma, Zhewei Yao, Amir Gholami, Michael W Mahoney, and Kurt Keutzer. 2020. Q-bert: Hessian based ultra low precision quantization of bert. In *Proceedings of the AAAI Conference on Artificial Intelligence*, volume 34, pages 8815–8821.
- Jascha Sohl-Dickstein, Eric Weiss, Niru Maheswaranathan, and Surya Ganguli. 2015. Deep unsupervised learning using nonequilibrium thermodynamics. In *International conference on machine learning*, pages 2256–2265. PMLR.
- Jiaming Song, Chenlin Meng, and Stefano Ermon. 2020. Denoising diffusion implicit models. *arXiv preprint arXiv:2010.02502*.
- Mingjie Sun, Zhuang Liu, Anna Bair, and J Zico Kolter. 2023. A simple and effective pruning approach for large language models. *arXiv preprint arXiv:2306.11695*.
- Yi-Lin Sung, Jaemin Cho, and Mohit Bansal. 2022. Vi-adapter: Parameter-efficient transfer learning for vision-and-language tasks. In *Proceedings of the IEEE/CVF Conference on Computer Vision and Pattern Recognition*, pages 5227–5237.
- Hugo Touvron, Thibaut Lavril, Gautier Izacard, Xavier Martinet, Marie-Anne Lachaux, Timothée Lacroix, Baptiste Rozière, Naman Goyal, Eric Hambro, Faisal Azhar, et al. 2023a. Llama: Open and efficient foundation language models. *arXiv preprint arXiv:2302.13971*.
- Hugo Touvron, Louis Martin, Kevin Stone, Peter Albert, Amjad Almahairi, Yasmine Babaei, Nikolay Bashlykov, Soumya Batra, Prajwal Bhargava, Shrubti Bhosale, et al. 2023b. Llama 2: Open foundation and fine-tuned chat models. *arXiv preprint arXiv:2307.09288*.
- Ashish Vaswani, Noam Shazeer, Niki Parmar, Jakob Uszkoreit, Llion Jones, Aidan N Gomez, Łukasz Kaiser, and Illia Polosukhin. 2017. Attention is all you need. *Advances in neural information processing systems*, 30.
- Alex Wang, Yada Pruksachatkun, Nikita Nangia, Amanpreet Singh, Julian Michael, Felix Hill, Omer Levy, and Samuel Bowman. 2019. **Superglue: A stickier benchmark for general-purpose language understanding systems**. In *Advances in Neural Information Processing Systems*, volume 32. Curran Associates, Inc.
- Alex Wang, Amanpreet Singh, Julian Michael, Felix Hill, Omer Levy, and Samuel Bowman. 2018. **GLUE: A multi-task benchmark and analysis platform for natural language understanding**. In *Proceedings of the 2018 EMNLP Workshop BlackboxNLP: Analyzing and Interpreting Neural Networks for NLP*, pages 353–355, Brussels, Belgium. Association for Computational Linguistics.
- Sinong Wang, Belinda Z Li, Madian Khabsa, Han Fang, and Hao Ma. 2020. Linformer: Self-attention with linear complexity. *arXiv preprint arXiv:2006.04768*.
- Xiuying Wei, Ruihao Gong, Yuhang Li, Xianglong Liu, and Fengwei Yu. 2022a. Qdrop: Randomly dropping quantization for extremely low-bit post-training quantization. *arXiv preprint arXiv:2203.05740*.
- Xiuying Wei, Yunchen Zhang, Yuhang Li, Xiangguo Zhang, Ruihao Gong, Jinyang Guo, and Xianglong Liu. 2023. Outlier suppression+: Accurate quantization of large language models by equivalent and optimal shifting and scaling. *arXiv preprint arXiv:2304.09145*.
- Xiuying Wei, Yunchen Zhang, Xiangguo Zhang, Ruihao Gong, Shanghang Zhang, Qi Zhang, Fengwei Yu, and Xianglong Liu. 2022b. Outlier suppression: Pushing the limit of low-bit transformer language models. *Advances in Neural Information Processing Systems*, 35:17402–17414.
- Guangxuan Xiao, Ji Lin, Mickael Seznec, Hao Wu, Julien Demouth, and Song Han. 2023. Smoothquant: Accurate and efficient post-training quantization for large language models. In *International Conference on Machine Learning*, pages 38087–38099. PMLR.
- Peng Xu, Wenqi Shao, Kaipeng Zhang, Peng Gao, Shuo Liu, Meng Lei, Fanqing Meng, Siyuan Huang, Yu Qiao, and Ping Luo. 2023. Lvlm-ehub: A comprehensive evaluation benchmark for large vision-language models. *arXiv preprint arXiv:2306.09265*.
- Jiwei Yang, Xu Shen, Jun Xing, Xinmei Tian, Houqiang Li, Bing Deng, Jianqiang Huang, and Xian-sheng Hua. 2019. Quantization networks. In *Proceedings of the IEEE/CVF Conference on Computer Vision and Pattern Recognition*, pages 7308–7316.
- Zhewei Yao, Cheng Li, Xiaoxia Wu, Stephen Youn, and Yuxiong He. 2023. A comprehensive study on

- post-training quantization for large language models. *arXiv preprint arXiv:2303.08302*.
- Zhewei Yao, Reza Yazdani Aminabadi, Minjia Zhang, Xiaoxia Wu, Conglong Li, and Yuxiong He. 2022. Zeroquant: Efficient and affordable post-training quantization for large-scale transformers. *Advances in Neural Information Processing Systems*, 35:27168–27183.
- Zhihang Yuan, Lin Niu, Jiawei Liu, Wenyu Liu, Xing-gang Wang, Yuzhang Shang, Guangyu Sun, Qiang Wu, Jiaxiang Wu, and Bingzhe Wu. 2023. Rptq: Reorder-based post-training quantization for large language models. *arXiv preprint arXiv:2304.01089*.
- Ali Hadi Zadeh, Isak Edo, Omar Mohamed Awad, and Andreas Moshovos. 2020. Gobo: Quantizing attention-based nlp models for low latency and energy efficient inference. In *2020 53rd Annual IEEE/ACM International Symposium on Microarchitecture (MICRO)*, pages 811–824. IEEE.
- Rowan Zellers, Ari Holtzman, Yonatan Bisk, Ali Farhadi, and Yejin Choi. 2019. Hellaswag: Can a machine really finish your sentence? In *Proceedings of the 57th Annual Meeting of the Association for Computational Linguistics*, pages 4791—4800.
- Renrui Zhang, Jiaming Han, Aojun Zhou, Xiangfei Hu, Shilin Yan, Pan Lu, Hongsheng Li, Peng Gao, and Yu Qiao. 2023a. Llama-adapter: Efficient fine-tuning of language models with zero-init attention. *arXiv preprint arXiv:2303.16199*.
- Susan Zhang, Stephen Roller, Naman Goyal, Mikel Artetxe, Moya Chen, Shuohui Chen, Christopher Dewan, Mona Diab, Xian Li, Xi Victoria Lin, et al. 2022a. Opt: Open pre-trained transformer language models. *arXiv preprint arXiv:2205.01068*.
- Susan Zhang, Stephen Roller, Naman Goyal, Mikel Artetxe, Moya Chen, Shuohui Chen, Christopher Dewan, Mona Diab, Xian Li, Xi Victoria Lin, et al. 2022b. Opt: Open pre-trained transformer language models. *arXiv preprint arXiv:2205.01068*.
- Yiyuan Zhang, Kaixiong Gong, Kaipeng Zhang, Hongsheng Li, Yu Qiao, Wanli Ouyang, and Xiangyu Yue. 2023b. Meta-transformer: A unified framework for multimodal learning. *arXiv preprint arXiv:2307.10802*.
- Lianmin Zheng, Wei-Lin Chiang, Ying Sheng, Siyuan Zhuang, Zhanghao Wu, Yonghao Zhuang, Zi Lin, Zhuohan Li, Dacheng Li, Eric Xing, et al. 2023. Judging llm-as-a-judge with mt-bench and chatbot arena. *arXiv preprint arXiv:2306.05685*.

A Appendix

In this appendix, we provide further details as follows:

- Sec. A.1: We provide the analysis of the expressiveness of the original models and the quantized counterparts.
- Sec. A.2: We provide the ablation studies of our techniques.
- Sec. A.2: We analyze the training time consumption of our techniques.
- Sec. A.4: We provide our complete results.

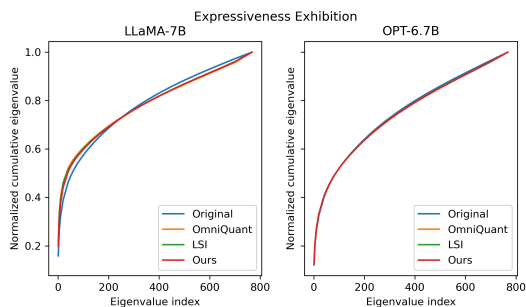


Figure 3: **Cumulative eigenvalue expressiveness** of the outputs of quantized LLaMA-7B and OPT-6.7B in W4A4 setting compared with the original models.

A.1 Expressiveness Analysis

In this section, we elaborate on the extensive experiments discussed in our main paper, focusing on comparing the expressiveness of quantized models to their original counterparts. We selected LLaMA-7B (Touvron et al., 2023a) and OPT-6.7B (Zhang et al., 2022b) as baseline models for generating text on WikiText (Merity et al., 2016) and C4 (Raffel et al., 2020), producing over 10,000 sentences with a length of 768 tokens each. We analyzed the final hidden states (a 2D matrix for each batch input) before they were input into the LM-Head (Brown et al., 2020; Touvron et al., 2023a; Zhang et al., 2022b), using singular value decomposition to assess each matrix. Our findings, illustrated in Fig. 3, reveal that changes in output expressiveness post-quantization are similar across both model families and independent of the quantization method used. Notably, for OPT-6.7B, the expressiveness remains almost unchanged after quantization.

In the case of LLaMA-7B, the minor variations observed primarily arise from how outliers are managed. Both OmniQuant (Shao et al., 2023) and our investigations indicate that weights in the LLaMA

family generally cluster within a narrow range but include some polarized outliers. The technique of Learnable Weight Clipping, introduced in (Shao et al., 2023), effectively addresses this issue by reducing the range of weight magnitudes. To validate this, we applied only the basic Learnable Equivalent Transformation during quantization and found that the expressiveness curve of the 'abridged version' of OmniQuant aligns perfectly with the original model's curve. This leads us to conclude that quantization does not significantly alter model properties, even in some low-bit settings, due to the inherent robustness of LLMs. Moreover, the slight increase in Perplexity (PPL) caused by quantized LLMs does not substantially affect their capabilities, as adjustments to the 'Temperature' parameter can be made to produce more 'categorical' responses. Therefore, the extraordinary results observed in the LSI series are more likely attributable to weight disturbances rather than fundamental changes in the model's core characteristics.

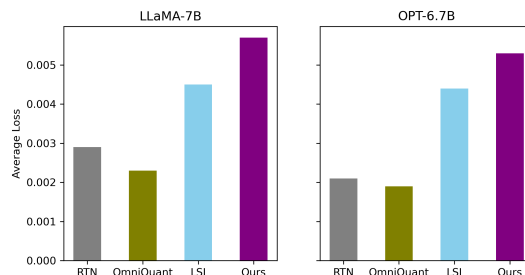


Figure 4: **Quantization loss magnitudes** of different quantization methods on LLaMA-7B in W4A4 settings.

To investigate the relationship between weight disturbances and the observed 'extraordinary' performances, we analyzed the quantization errors introduced by various methods. We calculated the absolute differences between the quantized weight matrices and their original counterparts (focusing solely on linear weight matrices) across the entire model and took their means. The results, depicted in Fig 4, indicate that the magnitudes of errors from LSI and our methods are significantly higher than those from Round to Nearest (RTN) and OmniQuant. Combining the insights from (Gao et al., 2023), we deduce that weight disturbances are the primary cause.

A.2 Ablation Study

In our ablation studies, we primarily examined the impact of varying the magnitude of n in our learnable parameter $\mathbf{I}^D \in \mathbb{R}^{(2n+1) \times b}$. The findings, pre-

Table 7: **DESV-only** quantization results

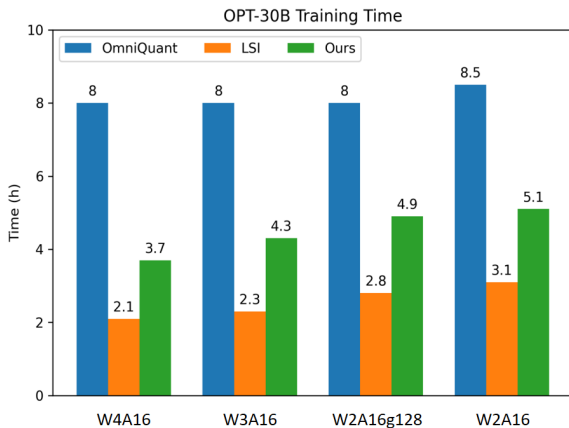
PPL		LLaMA-7b		OPT-2.7b			OPT-6.7b		
Task		WIKI	C4	WIKI	PT	C4	WIKI	PT	C4
W3A16g128	GPTQ (Frantar et al., 2022)	6.55	7.85	13.69	17.06	14.54	11.65	14.24	12.48
	LSI-only (Gao et al., 2024)	6.25	7.91	13.70	17.35	14.82	11.75	14.87	13.05
	DESV-only	6.23	7.96	13.52	17.14	14.63	11.54	14.48	12.81
W2A16g128	GPTQ (Frantar et al., 2022)	44.01	27.71	61.59	61.36	33.83	20.18	25.24	18.55
	LSI-only(Gao et al., 2024)	16.73	19.86	19.74	27.96	24.79	16.41	20.63	19.26
	DESV-only	14.82	15.91	18.95	25.31	22.07	14.87	19.12	17.11

Table 8: **Ablation studies** on the magnitude of n . Here, Num refers to the magnitude of n , and TT is the training time.

PPL		OPT-1.3B			
Task	Num	WIKI	PTB	C4	TT
W2A 16g128	100	21.39	31.88	24.75	39min
	50	21.91	31.27	25.16	32min
	200	20.93	30.90	24.58	53min
PPL		OPT-13B			
W2A 16g128	100	12.58	16.17	14.46	2h28min
	50	12.66	16.29	14.55	1h54min
	200	12.56	16.24	14.47	3h22min

sented in Table 8, suggest that $n = 50$ may not optimally utilize the potential of our techniques. For larger LLMs (especially for LLMs beyond 13B), increasing n beyond 100 yields diminishing returns, and excessively high values like $n = 200$ not only risk overfitting but also significantly extend the training duration. Generally, we suggest 100 as the best choice for n .

On the other hand, we also evaluated the exclusive implementation of our methods. We found that in higher-bit quantization settings, our methods demonstrate greater stability compared to LSI. Additionally, in low-bit settings, our methods generally exhibit no side effects, as detailed in Table 7.

Figure 5: **Training time comparisons** on OPT-30B using various quantization methods.

A.3 Training Time Consumption

We analyzed training time consumption as illustrated in Fig 5. Generally, for larger LLMs, our training duration is approximately 1.5 times longer than that of LSI. While our methods yield strong performances in low-bit settings, in higher-bit weight-only settings, such as W4A16 or W3A16g128, our results are comparable to those of LSI, making LSI sufficient for these scenarios. However, our methods exhibit greater stability in higher-bit weight-activation settings, except in the LLaMA families, where the weights are particularly sensitive.

A.4 Full Results

In this section, we provide a comprehensive presentation of our results across various datasets to complement the main paper. Specifically, the results include:

- Wiki perplexity with weight-only quantization in the LLaMA families (Table 9).
- PTB perplexity with weight-only quantization in OPT families (Table 10).
- C4 perplexity with weight-only quantization in OPT families (Table 11).

Table 9: **Weight-only** quantization results of LLaMA-1 Models (7B-30B).

LLaMA / PPL↓		LLaMA-7B		LLaMA-13B		LLaMA-30B	
Task		WIKI	C4	WIKI	C4	WIKI	C4
FP16	-	5.68	7.08	5.09	6.61	4.10	5.98
W2A16	GPTQ (Frantar et al., 2022)	2.1e3	689.13	5.5e3	2.5e3	499.75	169.80
	OmniQuant (Shao et al., 2023)	15.47	24.89	13.21	18.31	8.71	13.89
	LSI (Gao et al., 2024)	12.91	17.90	9.08	12.36	8.45	11.96
	Ours	10.48	15.20	8.90	12.21	8.37	11.91
W2A16 g128	GPTQ (Frantar et al., 2022)	44.01	27.71	15.60	15.29	10.92	11.93
	AWQ (Lin et al., 2023)	2.6e5	1.9e5	2.8e5	2.3e5	2.4e5	2.4e5
	OmniQuant (Shao et al., 2023)	9.72	12.97	7.93	10.36	7.12	9.36
	LSI (Gao et al., 2024)	10.52	13.79	10.11	12.24	7.46	10.02
Ours	9.26	12.53	7.76	10.19	7.01	9.32	
W2A16 g64	GPTQ (Frantar et al., 2022)	22.10	17.71	10.06	11.70	8.54	9.92
	AWQ (Lin et al., 2023)	2.5e5	2.8e5	2.7e5	2.2e5	2.3e5	2.3e5
	OmniQuant (Shao et al., 2023)	8.90	11.78	7.34	9.75	6.59	8.65
	LSI (Gao et al., 2024)	10.23	13.18	9.77	11.62	8.31	9.79
Ours	8.75	11.54	7.29	9.73	6.54	8.63	
W3A16	GPTQ (Frantar et al., 2022)	8.06	9.49	6.76	8.16	5.84	7.29
	AWQ (Lin et al., 2023)	11.88	13.26	7.45	9.13	10.07	12.67
	OmniQuant (Shao et al., 2023)	6.49	8.19	5.68	7.32	4.74	6.57
	LSI (Gao et al., 2024)	6.38	8.17	5.65	7.33	4.69	6.58
Ours	6.38	8.17	5.57	7.29	4.65	6.56	

Table 10: **PTB perplexity of Weight-only** quantization results in OPT models.

OPT / PPL↓		125M	1.3B	2.7B	6.7B	13B	30B	66B
FP16	-	32.54	16.96	15.11	13.08	12.33	11.84	11.36
W2A16 g128	GPTQ (Frantar et al., 2022)	655.17	130.88	61.36	25.24	20.46	15.15	323.23
	AWQ (Lin et al., 2023)	263.88	71.87	43.15	19.49	17.61	14.92	19.33
	OmniQuant (Shao et al., 2023)	126.49	34.33	25.28	18.92	16.74	14.51	139.17
	LSI (Gao et al., 2024)	92.60	32.26	24.39	18.71	16.44	14.27	116.21
Ours	84.08	31.88	23.44	18.43	16.17	14.13	97.32	
W2A16 g64	GPTQ (Frantar et al., 2022)	245.28	55.61	36.12	19.45	17.02	14.05	88.92
	AWQ (Lin et al., 2023)	143.18	41.19	25.08	18.00	15.83	14.92	15.72
	OmniQuant (Shao et al., 2023)	112.10	30.36	22.63	17.58	15.70	13.98	13.51
	LSI (Gao et al., 2024)	81.40	29.17	22.51	17.55	15.55	13.90	13.47
Ours	75.67	28.79	22.33	17.51	15.33	13.76	13.42	
W3A16	GPTQ (Frantar et al., 2022)	34.05	27.39	15.94	13.75	13.71	12.54	21.16
	AWQ (Lin et al., 2023)	80.73	33.20	224.11	18.46	35.45	66.68	3.4e3
	OmniQuant (Shao et al., 2023)	45.29	20.42	17.08	14.23	13.49	12.54	11.71
	LSI (Gao et al., 2024)	40.56	19.85	16.65	14.02	13.42	12.48	11.69
Ours	39.47	19.36	16.61	14.04	13.17	12.41	11.64	

Table 11: **C4 perplexity of Weight-only** quantization results in OPT models.

OPT / PPL↓		125M	1.3B	2.7B	6.7B	13B	30B	66B
FP16	-	24.60	14.72	13.16	11.74	11.19	10.69	10.69
W2A16 g128	GPTQ (Frantar et al., 2022)	597.66	60.88	33.83	18.55	16.34	12.89	598.81
	AWQ (Lin et al., 2023)	168.35	38.38	26.41	16.48	14.73	12.98	15.42
	OmniQuant (Shao et al., 2023)	80.10	27.33	21.11	16.67	14.92	13.12	73.83
	LSI (Gao et al., 2024)	64.17	25.76	20.61	16.28	14.66	13.00	66.25
Ours	59.18	24.75	20.10	16.01	14.46	12.88	56.37	
W2A16 g64	GPTQ (Frantar et al., 2022)	133.51	31.31	23.23	16.24	14.48	12.24	58.60
	AWQ (Lin et al., 2023)	90.19	27.34	20.01	15.20	13.90	12.43	13.31
	OmniQuant (Shao et al., 2023)	64.01	23.71	19.16	15.44	14.16	12.80	12.13
	LSI (Gao et al., 2024)	56.22	23.53	19.03	15.31	13.97	12.75	12.10
Ours	52.82	22.82	18.77	15.23	13.86	12.61	12.07	
W3A16	GPTQ (Frantar et al., 2022)	37.75	19.45	13.75	15.67	12.28	11.34	13.68
	AWQ (Lin et al., 2023)	55.73	24.56	154.49	15.84	23.71	55.01	3.8e3
	OmniQuant (Shao et al., 2023)	32.17	17.10	14.93	12.78	12.13	11.37	10.82
	LSI (Gao et al., 2024)	30.20	16.71	14.59	12.56	12.14	11.38	10.79
Ours	29.81	15.83	14.47	12.53	11.93	11.31	10.74	